Comparison of Radon Adsorption on Magnetite and Charcoal Activated Powder in Water

Vanja Radolić, Goran Šmit,* Marina Poje Sovilj, Josipa Namestnik

Josip Juraj Strossmayer University of Osijek, Department of Physics, Trg Ljudevita Gaja 6, HR-31000 Osijek, Croatia
* Corresponding author's e-mail address: gsmit@fizika.unios.hr

Abstract: Adsorption of radon in the artificially enriched water was investigated on magnetite, Fe_3O_4, and charcoal activated powder (activated carbon). Linear models of Langmuir, Freundlich and Dubinin-Radushkevich isotherms showed that radon adsorption on both adsorbents is a favourable chemical process, with weaker interactions with magnetite, that takes place forming a multilayer of adsorbed radon. The efficiency of both adsorbents was at a similar level but, because of the larger density and magnetic properties, magnetite could be more suitable in practical applications when smaller volume of adsorbent is advisable.

Keywords: magnetite, activated charcoal, radon, adsorption, water.
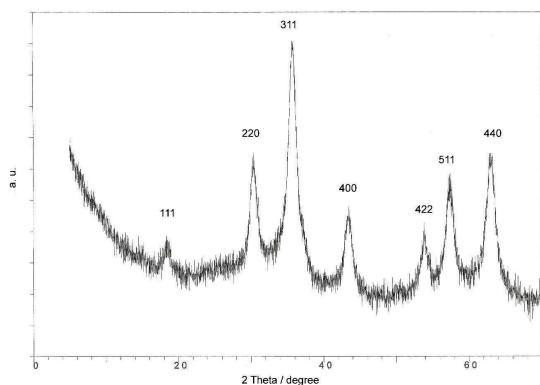
INTRODUCTION

RADON is a gas without colour, smell and taste from the noble gases group which means it is almost completely inert. Moreover, radon is the radioactive product of radium decay and, because they are both members of the uranium series, it easily diffuses into the environment around rocks rich with these two elements. In this way, it can enter through the foundations of the buildings into the rooms which people use for housing and work where in high concentrations it can be a danger to health. Radon can also be transferred by drinking water which can increase the incidence of lung and stomach cancers.[1] Higher levels of radon concentration have appeared in some groundwater supplies in North America and Europe.[2] Different granular activated carbon filtration methods and aeration systems were used and found to be very efficient in removing radon from individual and public water supplies, as well.[3,4] The disadvantage of appliance activated carbon for that purpose is the accumulation of radon in the filter and the growth of gamma-emitting radon products which produce the further problems in the disposal of used granular activated carbon. On the other hand, aeration does not have this problem, but it costs more. The aim of this work was to investigate the adsorption equilibrium of radon in artificially enriched water on magnetite as an alternative adsorbent, because of its magnetic property and large density, and parallel on charcoal activated powder in the same experimental conditions.

EXPERIMENTAL

Adsorbents

As adsorbents were used magnetite was prepared in our laboratory and charcoal activated powder QP (PanReac, Spain) was received. Magnetite was synthesized in our laboratory according to Schwertmann and Cornell.[5] Figure 1 is an X-ray diffractogram of so prepared magnetite which was taken on a Philips 3710 diffractometer operated at 40 kV and 40 mA using monochromatic Cu *K*α radiation. The range in 2θ from 5 to 70° was scanned at a speed of 0.02° s⁻¹ at room temperature. Observed well-resolved maxima at 2θ = 18°, 30°, 35°, 43°, 54°, 57° and 63°, which correspond to planes (111), (220), (311), (400), (422), (511) and (440), reveal pure and crystalline Fe_3O_4 particles.[6] The magnetic behaviour of Fe_3O_4 particles enables smooth solid-liquid separation at the end of the adsorption by a simple magnetic separation.[7]

Figure 1. XRD pattern of magnetite used as the adsorbent for radon in water.

Figure 2. Photographs of magnetic separation of Fe_3O_4 by an external magnet at the end of the adsorption.

Adsorption

The samples for the adsorption of radon in water on synthesized magnetite and charcoal activated powder were prepared using the radium solution method in a way that the final activities of the solutions were in the range from 30 to 500 Bq dm^{-3}. The certified radium standard, A(^{226}Ra) = 3731 ± 26 Bq from Czech Metrology Institute was used. 20 cm^3 of the diluted standard was transferred into a 20 cm^3 scintillation vial (high performance, low potassium, glass vials from Perkin Elmer) waiting approximately 30 days (more than 8 half-lives of radon) for reaching secular equilibrium between radium and radon. So prepared samples are acidic because of carrier solution of radium standard consists of 1 g dm^{-3} BaCl$_2$ and 10 g dm^{-3} HCl in distilled water. pH of prepared samples was measured by HandyLab 100 pH-meter manufactured by SI Analytics, GmbH, Germany. The obtained results were in the pH-range from 1.6 to 2.5 depending on the radium standard volume used in targeting radon concentrations. The adjustment of pH values between 6.52 and 7.45 in samples was performed with 0.125 M NaOH immediately before adding adsorbent to vials. After reaching the wanted pH, 0.03 g of magnetite or charcoal activated powder was added to each sample and shaken for 10 minutes at a constant temperature (298.15 K). The adsorption equilibrium was usually reached already after 5 minutes. The separation of magnetite at the end of the adsorption from solution was performed by an external magnet (Figure 2) while in the case of activated charcoal it was by filtration using Whatman No. 41 filter paper. 10 cm^3 of transparent radon sample was added to 10 cm^3 of not-miscible scintillation cocktail Ultima Gold F which was earlier prepared in a new scintillation vial. The background samples were prepared by using 10 cm^3 of distilled water transferred to 10 cm^3 of scintillation cocktail. The radon concentrations in water samples were measured by the liquid scintillation counter TriCarb 2900 and the obtained spectra were acquired and analysed by the SpectraView software (Perkin Elmer). The liquid scintillation instrument has its background reduction system around the detector which consists of a passive shield made of lead. Radon concentration in the water sample, c(Rn) / Bq dm^{-3} and 2σ uncertainty (95 % CI) were obtained by using the following equations:

$$c(\text{Rn}) = \frac{G - B}{CF \cdot D \cdot V} \quad (1)$$

$$2\sigma = \frac{2\left(\dfrac{G}{T_G} + \dfrac{B}{T_B}\right)^{1/2}}{CF \cdot D \cdot V} \quad (2)$$

where G / cpm is the gross counting rate of the sample, B/ cpm is the background counting rate, D ($e^{-\lambda t}$) is the decay correction factor for radon between the time of preparing samples to the midpoint of the counting period, CF is calibration factor, V / dm^3 is the volume of the water sample and T_B and T_G are time duration of the background and sample count / min, respectively. In our case, the measurement times for both, samples and background were 60 minutes, sample volumes were 10 cm^3, and calibration factor CF = (275 ± 2) cpm Bq^{-1}. The calibration was performed according to the ISO 13164-4:2015 procedure and a linear calibration curve (R^2 = 0.999) over different ranges of activity concentrations is obtained.

The measured radon concentrations, c(Rn) / Bq dm^{-3} were converted to amount concentration, $c = n\ V^{-1}$ / mol dm^{-3} in the following way. The amount of substance (radon), n is defined as

$$n = \frac{m}{M} \quad (3)$$

where m is the mass of radon / g, and M is the molar mass of radon (M = 222 g mol^{-1}). The mass of radon can be determined from

$$m = \frac{A}{SA} \qquad (4)$$

where A is the activity of radon / Bq and SA is the specific activity / Bq g^{-1} which is equal to 5.7 · 10^{15} Bq g^{-1} according to the relation

$$SA = \frac{N_A \cdot \lambda}{M} \qquad (5)$$

where N_A is Avogadro constant (N_A = 6.022 · 10^{23} mol^{-1}) and λ is decay constant of radon (λ = 2.1 · 10^{-6} s^{-1}). The activity of radon in the water sample, A can be expressed as c(Rn) · V, where V is a volume of sample (10 cm^3). Therefore,

$$c = \frac{c(\text{Rn})}{N_A \cdot \lambda} \qquad (6)$$

## RESULTS AND DISCUSSION

Isotherm Models

Isotherm models provide the information about sorts of bonding between adsorbates and adsorbents and theoretical maximum adsorption capacity based on the final adsorbed quantity of adsorbate per unit of adsorbent mass concerning its remaining concentration at the end of adsorption.

The adsorbed amount of radon in the equilibrium, q_e (mol g^{-1}), is determined as:[7]

$$q_e = \frac{(c_0 - c_e) \cdot V_S}{m_A} \qquad (7)$$

where c_0 / mol dm^{-3} is the initial concentration of radon in the water, c_e / mol dm^{-3} is the concentration of radon in the water at equilibrium, V_S / dm^3 is the volume of the system and m_A / g is the mass of adsorbent.

Figure 3 depicts experimental adsorption isotherms as the dependence of radon uptake at magnetite and
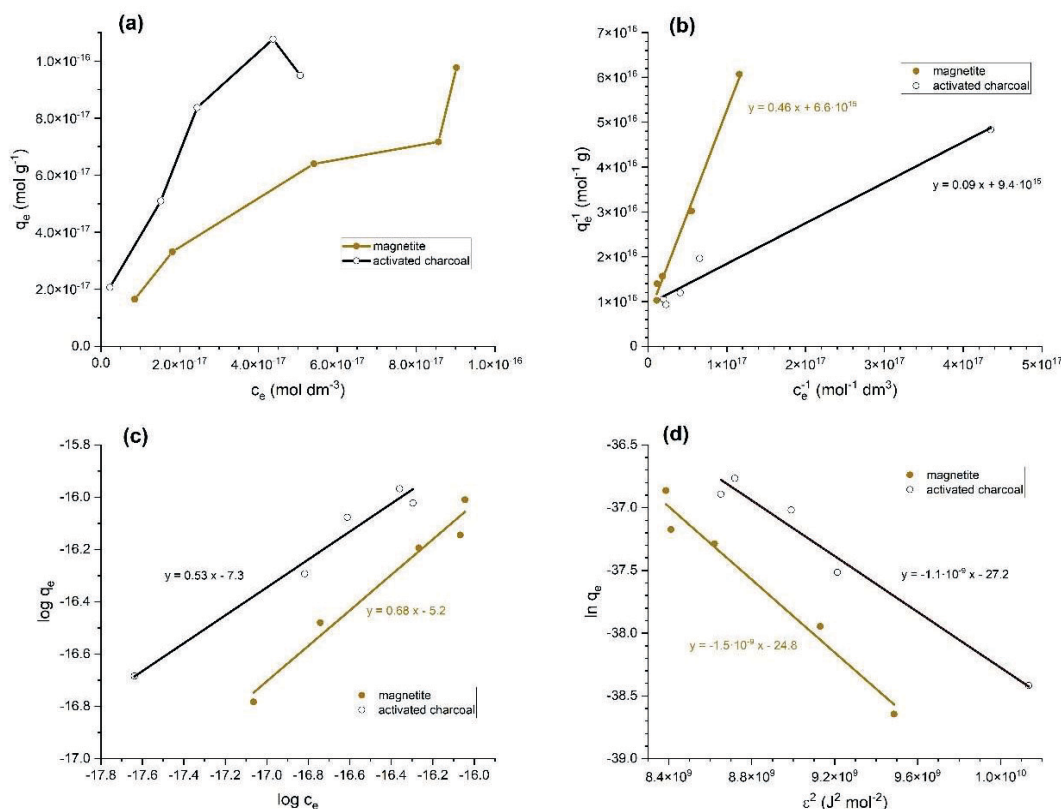
Figure 3. Experimental adsorption isotherms as the dependence of radon uptake at magnetite and charcoal activated powder of equilibrium radon concentrations in water (a), Langmuir linear plots (b), Freundlich linear plots (c), Dubinin-Radushkevich linear plots (d).

charcoal activated powder of equilibrium radon concentrations in water (a), and linear plots of those data according to Langmuir (b), Freundlich (c) and Dubinin-Radushkevich (d) linear models.

As can be seen, the adsorption isotherm for magnetite has the shape of a more frequently L isotherm ("Langmuir type"), subclass 3, with a characteristic initial increase of the adsorbed radon with an increase of initial radon concentration in the water followed by saturation, caused by limited free sites, and forming an adsorbed monolayer. Then appears competition among particles in liquid phase for available sites. It is characteristic of systems with very polar adsorbent and adsorbate. In subclass 3, after the plateau, are formed more adsorbed layers (multilayer) indicating some interparticle interaction between adsorbed adsorbent and adsorbent in solution.[8]

Isotherm for activated charcoal could be described, in the same manner, as the S curve because after an inclined slope appears a curvature followed by an uprising which could be explained by the change of particles orientation during adsorption. The S type isotherms are characteristic for adsorptions where adsorbent has a low affinity for adsorbate but at higher concentrations, other particles can easier adsorb themselves forming multilayer. More precisely, this S curve can be associated with subclasses Smx because the first inflexion was followed by the fall in slope which could be interpreted only with stronger adsorbate-adsorbate attraction in comparison to forces between adsorbent and adsorbate which occurs with an increase of concentration. A similar observation was reported during the adsorption of phenols on activated carbon[9] but with a total fall in the slope. Anyway, it is possible the curve rises again after the first fall[10] and even more times with successive maxima (mxmx).

Table 1. Parameters of linear Langmuir, Freundlich and Dubinin-Radushkevich adsorption isotherm models.

| Isotherm model	Parameter	Magnetite	Charcoal activated powder
Langmuir	q_{max} / mol g^{-1}	$1.5152 \cdot 10^{-16}$	$1.0638 \cdot 10^{-16}$
	K_L / mol^{-1} dm^3	$1.4347 \cdot 10^{16}$	$1.0445 \cdot 10^{17}$
	R_L	$0.6765 - 0.2274$	$0.2231 - 0.0466$
	R^2	0.9940	0.9766
Freundlich	$1/n_F$	0.68	0.53
	K_F / mol g^{-1}	$6.3096 \cdot 10^{-6}$	$5.3703 \cdot 10^{-8}$
	R^2	0.9703	0.9715
Dubinin-Radushkevich	q_{max} / mol g^{-1}	$1.6963 \cdot 10^{-11}$	$1.5873 \cdot 10^{-12}$
	E / J mol^{-1}	18257.419	22360.680
	R^2	0.9715	0.9715

Table 1 presents the parameters of linear Langmuir, Freundlich and Dubinin-Radushkevich adsorption isotherm models.

Langmuir model is theoretically an idealized form of adsorption because it is valid for the dynamic equilibrium of the adsorption-desorption process on a homogenous surface which means that all adsorption sites on the surface have the same affinity for adsorbate. As a result, the adsorption energy is the same for all sites and independent of surface coverage because there is no interaction between adjacent adsorbed particles. When the adsorbate particle occupies such a site there is no further adsorption at that same site. Adsorption ends with the formation of only one layer of adsorbate on the surface of the adsorbent: it is monolayer adsorption.

The linear form used for Langmuir isotherm modelling was:[11]

$$\frac{1}{q_e} = \frac{1}{q_{max} \cdot K_L} \cdot \frac{1}{c_e} + \frac{1}{q_{max}} \tag{8}$$

where q_{max} / mol g^{-1} is the maximum adsorption capacity of the monolayer and K_L / mol^{-1} dm^3 is Langmuir constant which could be assumed as equilibrium constant K because it is the actual constant for dynamic equilibrium of:[12]

$$A(g) + M(surface) \rightleftarrows AM(surface)$$
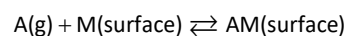
with rate constants k_a for adsorption and k_d for desorption. Hence:

$$K = \frac{k_a}{k_d} \tag{9}$$

As can be seen, values of q_{max} are almost identical and large values of K_L suggest rather a favourable adsorption on both adsorbents.

This is also confirmed by an important feature of the Langmuir isotherm known as the separation factor, R_L:

$$R_L = \frac{1}{1 + K_L \cdot c_0} \tag{10}$$

Namely, R_L values can very simply characterize adsorption as:[7]

- Favourable adsorption: $0 < R_L < 1$,
- Unfavourable adsorption: $R_L > 1$,
- Irreversible adsorption: $R_L = 0$,
- Linear adsorption: $R_L = 1$.

Values are significantly closer to zero in the case of activated charcoal, which indicates stronger interactions with radon[13] in comparison with magnetite. Also, higher R_L

at lower concentrations in both cases implies that adsorption is favourable at lower concentrations,[14] especially on magnetite, considering the difference between the first and the last value.

Freundlich isotherm is quite the opposite to Langmuir model. It has an empirical approach to heterogeneous surfaces which means that not all adsorption sites have the same affinity for adsorbate, and adsorption itself is reversible. Consequently, the adsorption energy depends on the surface coverage because there are interactions among adsorbed particles. The binding intensity is inverse to the degree of coverage while the adsorption energy drops exponentially as it approaches equilibrium. This isotherm, which is suitable also for multilayer adsorption, looks in linear form:[7]

$$\log q_e = \log K_F + \frac{1}{n_F} \cdot \log c_e \tag{11}$$

where K_F / mol g^{-1} presents the adsorption capacity of the system with the possibility of forming a multilayer. If $n_F^{-1} = 1$ it suggests that the adsorption process is linear; meaning that q_e is proportional to the initial concentration. Otherwise, $n_F^{-1} > 1$ implies adsorption as a favourable physical process and $n_F^{-1} < 1$ adsorption is a chemical process.

Values of K_F in comparison with q_{max} values from Langmuir model assume forming of multilayer in both cases, with a greater capacity on magnetite. Looking at n_F^{-1}, one can conclude that adsorption is chemical over magnetite and also over activated charcoal, but that latter value is smaller implying stronger bonding which is in accordance with the results of R_L.

Dubinin-Radushkevich model is also empirical but similar to Langmuir isotherm with the main difference in the assumption that adsorption can take place on heterogeneous as well as homogeneous surfaces. It is related to the heterogeneity of energies close to the surface of the adsorbent and a multilayer character is suggested. In this model, as an expression of the surface working function, is introduced the Polanyi potential, ε / J mol^{-1}:

$$\varepsilon = RT \ln\left(1 + \frac{1}{c_e}\right) \tag{12}$$

where R is the gas constant (8,314 J K^{-1} mol^{-1}) and T / K is the temperature. In the Dubinin-Radushkevich linear model:[15,16]

$$\ln q_e = \ln q_{max} - K_{DR} \cdot \varepsilon^2 \tag{13}$$

where K_{DR} / J^{-2} mol^2 is the Dubinin-Radushkevich constant related to the mean free energy of adsorption per mole of the adsorbate E / J mol^{-1} as:

$$E = \frac{1}{\sqrt{(-2K_{DR})}} \tag{14}$$

The value of E may offer a conclusion about the adsorption mechanism. When it is in the range of 1–8 kJ mol^{-1}, it supposes physical adsorption. The value of E between 8 and 16 kJ mol^{-1} is attributed to the adsorption process that takes place by the chemical ion-exchange mechanism, while E greater than 16 kJ mol^{-1} indicates chemisorption. So, in both occasions, chemical adsorption occurs but is more intensively over charcoal activated carbon as it is confirmed also with R_L values.

At this level, it is difficult to assume any kind of bonding that radon forms with magnetite and charcoal activated powder in water.

On the other hand, magnetite has surface neutral hydroxyl groups (–OH), that may provide, especially after hydration, positive and/or negative charges as –OH$_2^+$ and –O$^-$ ions, in dependence of pH, which could be involved in chemisorption. Even more, at any pH it is always possible that neutral, positive and negative sites appear together.[17] Besides that, magnetite has Fe(II) and Fe(III) ions which could be involved in redox reactions like it is in the reduction of Cr(VI) in Cr(III) ion.[6]

Charcoal activated powder has also well-known functional groups, such as C – C, C– O, C – N, C – H, O – H[18] which enable chemisorption.

So, both investigated adsorbents can participate in chemisorption and examples are magnetite in the adsorption of H$_2$ and CO$_2$ during the reduction of CO$_2$[19] and powdered activated carbon in covalently bounding of perfluorooctanoic acid aqueous solution where oxidized sites of the carbon were involved in the coupling process.[20]

CONCLUSION

Analysis of isotherm models confirms that radon adsorption on magnetite, Fe$_3$O$_4$, and charcoal activated powder is a favourable chemical process, with weaker interactions on magnetite, that takes place forming a multilayer of adsorbed radon.

Adsorption capacity is greater on the same mass of magnetite in comparison to charcoal activated powder.

Magnetite has great potential as a radon adsorbent in water because of its magnetic property and larger density considering charcoal activated powder. Because of that, in practical applications where the volume of adsorbent plays an important role in the adsorption process and the disposal of used adsorbent, magnetite could be more appropriate for radon adsorption in water than granular activated carbon.

REFERENCES

[1]　A. I. Alabdulaʾaly, H. B. Maghrawy, *J. Radioanal. Nucl. Chem.* **1999**, *241*, 3–9. https://doi.org/10.1007/BF02347282

[2]　A. I. Alabdulaʾaly, H. B. Maghrawy, *J. Radioanal. Nucl. Chem.* **2011**, *287*, 77–85. https://doi.org/10.1007/s10967-010-0804-1

[3]　J. D. Lowry, W. F. Brutsaert, T. McEnerney, C. Molk, *J. Am. Water Works Assoc.* **1987**, *79*, 162–169. https://doi.org/10.1002/j.1551-8833.1987.tb02829.x

[4]　S. D. Jastaniah, B. Z. Shakhreet, H. Y. Abbas, A. M. Elkhadir, S. M. Bafaraj, *Open J. of Biophys.* **2014**, *4*, 7–12. http://dx.doi.org/10.4236/ojbiphy.2014.41002

[5]　U. Schwertmann, R. M. Cornell, *Iron Oxides in the Laboratory: Preparation and Characterization*, VCH, Weinheim, **1991**, p. 112.

[6]　S. A. Elfeky, S. E. Mahmoud, A. F. Youssef, *J. Adv. Res.* 2017, 8, 435–443. https://doi.org/10.1016/j.jare.2017.06.002

[7]　M. Iram, C. Guo, Y. Guan, A. Ishfaq, H. Liu, *J. Hazard. Mater.* **2010**, *181*, 1039–1050. https://doi.org/10.1016/j.jhazmat.2010.05.119

[8]　J. S. Piccin, T. R. S. Cadaval Jr., L. A. A. de Pinto, G. L. Dotto in *Adsorption Processes for Water Treatment and Purification* (Eds.: A. Bonilla-Petriciolet, D. I. Mendoza-Castillo, H. E. Reynel-Ávila), Springer, Cham, **2017**, pp. 19–51. https://doi.org/10.1007/978-3-319-58136-1

[9]　R. B. Lekene Ngouateu, P. M. A. Kouoh Sone, J. Ndi Nsami, D. Kouotou, P. D. Belibi Belibi, J. Ketcha Mbadcam, *Int. J. Curr. Res. Rev.* **2015**, *7*, 1. http://dx.doi.org/10.14419/ijbas.v4i3.4721

[10]　C. H. Giles, T. H. MacEwan, S. N. Nakhwa, D. Smith, *J. Chem. Soc. (Resumed)* **1960**, 3973–3993. https://doi.org/10.1039/JR9600003973

[11]　R. S. Bose, S. Dey, S. Saha, C. K. Ghosh, M. G. Chaudhuri, *Sustain. Water Resour. Manag.* **2016**, *2*, 143–159. https://doi.org/10.1007/s40899-016-0045-8

[12]　P. Atkins, J. de Paula, Atkins' Physical Chemistry, Oxford University Press, Oxford, **2010**, p. 890.

[13]　M. Kumar, R. Tamilarasan, *Polish J. Chem. Tech.* **2013**, *15*, 29. https://doi.org/10.2478/pjct-2013-0021

[14]　M. Belhachemi, F. Addoun, *Appl. Water Sci.* **2011**, *1*, 111–117. https://doi.org/10.1007/s13201-011-0014-1

[15]　F. Yu, J. Chen, L. Chen, J. Huai, W. Gong, Z. Yuan, J. Wang, J. Ma, *J. Colloid Interface Sci.* **2012**, *378*, 175–183. https://doi.org/10.1016/j.jcis.2012.04.024

[16]　A. Babkin, I. Burakova, A. Burakov, D. Kurnosov, E. Galunin, A. Tkachev, I. Ali, *IOP Conf. Ser.: Mater. Sci. Eng.* **2019**, *693*, 012045. https://doi.org/10.1088/1757-899X/693/1/012029

[17]　A. J. Herbillon in *Iron in Soils and Clay Minerals* (Eds.: J. V. Stucki, B. A. Goodman, U. Schwertmann), Springer, Dordrecht, **1988**, pp. 251–266. https://doi.org/10.1088/1757-899X/693/1/012029

[18]　C. A. Sáenz-Alanís, R. B. García-Reyes, E. Soto-Regaldo, A. García-González, *Adsorp. Sci. Technol*. **2017**, *35*, 789–805. https://doi.org/10.1177/0263617416684517

[19]　Y. Zhu, X. Zhang, K. Koh, L. Kovarik, J. L. Fulton, K. M. Rosso, O. Y. Gutiérrez, *Nat. Commun*. **2020**, *11*, 1. https://doi.org/10.1038/s41467-020-16830-4

[20]　B. Sun, J. Ma, D. L. Sedlak, *Environ. Sci. Technol*. **2016**, *50*, 7618–7624. https://doi.org/10.1021/acs.est.6b00411